Canrea Journal: Food Technology, Nutritions, and Culinary, 2025; 8 (2): 425–447 OPEN ACCESS

e-ISSN : 2621-9468

Type of the Paper (Article)

In silico approaches to analyse *Acanthus ilicifolius* leaves extract as α-glucosidase and α-amylase inhibitors

Yunita Eka Puspitasari[1*], Yunita Aminatus Sholichah[1], Naufal Rakha Defransyah[1], Titik Dwi Sulistiyati[1], Luthfi Ari Prihanto[1], Irenia Paulin Hutapea[1], Angga Wira Perdana[1], Ahmad Fauzi[2,3], and Hardoko Hardoko[1]

[1] Department of Fish Product Technology, Faculty of Fisheries and Marine Sciences, Universitas Brawijaya, Jl. Veteran Malang, 65145, Indonesia
[2] Department of Veterinary Pathology and Microbiology, Faculty of Veterinary Medicine, Universiti Putra Malaysia UPM, Serdang 43400, Selangor, Malaysia
[3] Department of Clinical Pathology, Faculty of Veterinary Medicine, University of Brawijaya, Malang East Java 65141, Indonesia

Abstract

α-glucosidase and α-amylase inhibitors were employed as treatments for type II diabetes. Acarbose, a commonly used commercial medicine for diabetes, has been widely utilized. However, it is associated with gastrointestinal adverse effects. Hence, the investigation of mangrove plants as potential sources of α-glucosidase and α-amylase inhibitors has garnered significant interest. In Indonesia, the leaves of the *Acanthus ilicifolius* shrub, commonly known as mangrove, are processed into black and green tea. Nevertheless, the investigation of phytochemical substances and their potential as antidiabetic agents has not yet been conducted. Hence, the objective of this study was to determine the phytochemical constituents of the extract obtained from *A. ilicifolius* mangrove leaves and to evaluate its inhibitory effects on α-glucosidase and α-amylase enzymes using computational methods. The investigations consisted of two steps: the identification of phytochemical substances and the analysis of molecular docking between receptor α-glucosidase (PDB ID: 3A4A) and α-amylase (PDB ID: 4GQR). *A. ilicifolius* leaf extract contains a variety of phytochemical compounds, including terpenoids (oleanolic acid), steroid (flurandrenolide), flavonoid (corymboside, scutellarin, apigenin 7-O-glucuronide, luteolin, glycitein, apigenin, 4-coumaric acid, were identified in this study. In binding interactions with α-glucosidase, three compounds—reserpine (-10 kcal/mol), scuttelarin (-9.9 kcal/mol), and apigenin-7-glucuronide (-9.9 kcal/mol)—establish a higher energy binding in comparison to the other ligands. Four compounds extracted from the leaves of *A. ilicifolius*, particularly corymboside, apigenin-7-glucuronide, scutellarin, and oleanolic acid, exhibit greater molecular affinity in their interaction with α-amylase. As a result, it can be deduced that the leaf extract of *A. ilicifolius* exhibits significant inhibitory activity against α-glucosidase and α-amylase via in silico techniques. As a result, it can be deduced that the leaf extract of *A. ilicifolius* exhibits significant inhibitory activity against α-glucosidase and α-amylase via *in silico* methods.

Article History
Received November 8, 2023
Accepted November 25, 2025
Published December 31, 2025

Keywords
Acanthus ilicifolius, α-glucosidase, α-amylase, Diabetes, *Teh Jeruju*

* Correspondence : **Yunita Eka Puspitasari** yunita_ep@ub.ac.id

ISSN 2621-9468 online, DOI 10.20956/canrea.v8i2.1165

1. Introduction

α-glucosidase plays a pivotal role in the process of carbohydrate digestion by breaking down dietary starches and sugars into glucose. This glucose is then absorbed and delivered into the bloodstream through glucose transporters. The increase in blood glucose level serves as the initial indication of type-2 diabetes mellitus (T2DM). α-glucosidase is a crucial factor in the human body that regulates postprandial glycaemia by slowing down the breakdown of carbohydrates and the absorption of glucose in the intestine. This is because only single sugar molecules are absorbed in the intestines (1). The administration of α-glucosidase inhibitors, such as acarbose, miglitol, and acarbose, in the form of oral medicines, is widely regarded as the most effective treatment for regulating blood glucose levels. These oral medications have been extensively used and are commercially available (2). α-glucosidase inhibitors were administered as monotherapy along with combination therapy with other antidiabetic agents (3). Therefore, it is crucial to investigate the development of novel α-glucosidase inhibitors that are both safer and have fewer side effects for the treatment of T2DM.

The discovery of natural compounds with α-glucosidase inhibitory properties from both terrestrial and marine plants has garnered significant interest from researchers. Previous research have assessed terrestrial plants as potential sources of α-glucosidase inhibitors, which encompassed: *Senegalia catechu* (4), *Hancornia speciosa* (5), *Acer* sp (6)*Ferula narthex* (7), partridge tea of *Mallotus furetinus* (8), *Zizyphus rugosa* (9), and marine plant such as *Fucus vesiculosus* (10), *Ascophyllum nodosum, Laminaria digitata*, *Grateloupia elliptica* (11). Specifically, indigenous communities have utilized mangrove plants due to their nutritional and therapeutic properties. The following vegetables were found in the mangrove area: *Lumnitzera racemose Willd, Acanthus illicifolius L., Rhizophora apiculata Bl., Ceriops tagal (Perr), Ceriops decandra (Griff.) Ding Hou, Bruguiera glymnorrhiza (L.) Savigny, B. parviflora, R. mucronata, B. cylindrica, Nypa fruticans, Sonneratia caseolaris (L.) Engl* (12,13). The previous study conducted on diverse species has shown that tannins, alkaloids, and steroids are major compounds found in mangroves, as revealed by phytochemical screenings (13). Multiple studies have demonstrated that *Rhizophora mucronata*, *Sonneratia alba*, and *Ceriops decandra* have been identified as inhibitors of α-glucosidase and α-amylase (14–19).

Acanthus ilicifolius, one of mangrove species, have been used as herbal medicine and also as functional beverage (20). The leaves of *A. ilicifolius* have been produced as both black and green tea in UKM. Tani Mangrove Surabaya, East Java, Indonesia. Nevertheless, the investigation into phytochemical substances and their biological efficacy as antidiabetic agents was restricted. Multiple components of *Acanthus sp.* have been examined, including the leaves, roots, barks, and stems. Secondary metabolites have been identified from *Acanthus sp.* leaves including benzoxaxinoid glucosides (21), lignan glucosides (22); megastigmane glucoside (23); cyclolignan lignan (24); ,11-epoxymegastigmane glucoside dan megastigmane glucosides, (6S, 9S)-roseoside (25); 2-benzoxazolinone, 2-hydroxy-2H-1,4-benzoxazin-3(4H)-one, (2R)-2-O-β-$_D$-glucopyranosyl-2H-1,4-benzox azin-3(4H)-one, (2R)-2-O-β-$_D$-glucopyranosyl-4-hydroxy-2H-1,4-benzoxazin-3(4H)-one(4),(2R)-2-O-b-D-glucopyranosyl-7-hydroxy-2H-1,4-benzoxazin-3(4H)-one, lyoniside, 3'-methoxy-luteolin-7-O-β-D-glucopyranoside, β-sitosterol-3-O-β-$_D$-glucopyranoside, stigmasterol octadecanoate, β-sitosterol octadecanoate, stigmasterol-3-O- b-D-glucopyranoside (26); pyridol[1,2-a]indole alkaloid, acanthiline A dan aurantiamide acetate (27). In addition, it was reported that the plants contained phenylethanoid glycoside (ilicifolioside A), aliphatic alcohol glycoside (ilicifolioside B); campneoside I, acteoside, phenylethyl-*O*-β-$_D$-glucopyranosyl-(1→2)-β-$_D$-

glucopyranoside, castanoside E, castanoside F(28); ilicifolioside C, (*Z*)-4-coumaric acid glycosides, (*Z*)-4-coumaric acid 4-*O*-*β*-*D*-glucopyranoside, (*Z*)-4-coumaric acid 4-*O*-*β*-$_D$-apiofuranosyl-(1"→2')-glucopyranoside (29). Flavonoids have been extensively studied and discovered as natural inhibitors of α-glucosidase. These compounds, obtained from functional foods or herbal medication, have a low toxicity level, making them safe for human intake.

Antidiabetes activities of *A. ilicifolius* have been reported. Administration methanol extract of *A. ilicifolius* fruit 22.4 mg/kg bw for 14 days (30), ethanol extract of *A. ilicifolius* leaves 22.4 mg/kg bw (31); methanolic extract of *A. polystachus* 400 mg/kg bw for 28 days (32) decreased blood glucose level in diabetic rats. Methanolic extract of *A. montanus* leaves inhibited α-glucosidase activity IC_{50} 1.65±0.02 mg/mL and α-amylase IC_{50} 2.87±0.02 mg/mL (33). Ethanol extract of *A. ebracteatus* 25 µg/mL inhibited α-glucosidase activity 21.10±3.01 % and α-amilase 43.61±3.85 % (34). Nevertheless, there is a lack of research investigating the inhibitory effects of *A. ilicifolius* on α-glucosidase and α -amylase. For this reason, *in silico* methods were utilized to test the inhibitory effects of *A. ilicifolius* leaf extract on α-glucosidase and α-amylase.

2. Materials and Methods

2.1. Materials

The second, third, and fourth shoots of *A. ilicifolius* leaves were collected at Clungup Mangrove Conservation, located in Malang, Indonesia. The plant material was recognized at Materia Medika, Batu, Indonesia, with the reference number 074/129/102.20-A/2022. The research method was descriptive. The extract was obtained from a subsequent extraction method and utilized three solvents with various polarities, including n-hexane, ethyl-acetate, and methanol (pa) (Smart-Lab, Tangerang, Indonesia).

2.2. Methods

2.2.1. Preparation of *A. ilicifolius* Leaves Extract

The plant material was dried under the sun for approximately 4-5 days, and it was indicated that the moisture content was less than 8%. The dried leaves was milled and sieved to obtain fine powder leaves. The dried powder were extracted using a maceration extraction method, where they were soaked for three consecutive 24-hour periods. The powder leaves were extracted using a maceration extraction method, where they were soaked for three consecutive 24-hour periods. The powdered *A. ilicifolius* (15 g) were soaked in n-hexane for three days (3 days x225 mL). This process resulted in a residue and a filtrate. The residue underwent maceration with ethyl acetate (3 days x225 mL), followed by filtration. The sample was treated with methanol (3 days x225 mL) and subsequently filtered to separate the methanol filtrate. The ethyl acetate and methanol filtrate were concentrated using a vacuum evaporator to obtain the ethyl acetate extract and methanol extract, respectively. The two extracts were stored at a temperature of 4°C.

2.2.2. LC-HRMS Analysis

The identification of compounds in the ethyl acetate and methanolic extract was performed using LC-HRMS. N-hexane was not considered due to its lipophilic nature. An analysis was conducted using LC-HRMS with the HPLC-Thermo Scientific Dionex Ultimate 3000 RSLC nano, which was equipped with a micro flow meter. The mobile phase consists of two components: A mixture of water and 0.1% formic acid, and a mixture of acetonitrile and

0.1% formic acid. A chromatography column with dimensions of 50 x 1 mm and particle size of 1.9 µ was utilized to separate the phytochemical compounds. The flow rate was established at a rate of 40 µL/min. The mass spectra were obtained using the Thermo Scientific Q Exactive instrument in positive ion mode for a duration of 30 minutes. The full scan resolution was set at 70,000.

2.2.3. Drug-likeness and Toxicity Analysis

The drug-likeness properties of *A. ilicifolius* leaves were assessed using Lipinski's rule and the SwissADME database to predict models for physicochemical properties, pharmacokinetics, drug-likeness and medicinal chemistry friendliness (35). In addition, the toxicity level and LD_{50} were predicted using the Protox tool (36,37).

2.3. Molecular Interaction Analysis

2.3.1. Ligand Preparation

The 3D structure of the Ligand was obtained by downloading it in SDF format from the PubChem database (https://pubchem.ncbi.nlm.nih.gov). The native ligands, NAG and MYC, were obtained in SDF format from the Protein Data Bank (https://www.rcsb.org/). Furthermore, the molecular composition of ligand control, specifically acarbose, miglitol, and voglibose, was obtained in SDF format from the PubChem database (https://pubchem.ncbi.nlm.nih.gov).

2.3.2. Protein Preparation

The crystal structures of α-glucosidase and α-amylase were obtained from the Protein Data Bank (PDB ID: 3A4A and PDB ID: 4GQR) (https://www.rcsb.org/) respectively. In addition, the ligands and water molecules were eliminated, and polar hydrogen was introduced to the protein receptor using Biovia Discovery Studio 2019.

2.3.3. Molecular Docking

The ligands and receptor (PDB ID: 3A4A and PDB ID: 4GQR) were subjected to molecular docking using AutoDock in PyRx software (35) to examine the chemical interaction and binding energy between them. The ligands comprised a molecule derived from the extract of *A. ilicifolius* leaves, as well as control ligands including acarbose, miglitol, and voglibose. Additionally, a native ligand was included. Furthermore, the ligands were supplemented, so reducing the energy of the ligand, and subsequently transformed from SDF format to PDBQT format using Open Babel. The grid box dimensions for protein α-glucosidase and α-amylase were defined as follows: the center coordinates for α-glucosidase were x=21.2711, y=-0.7586, z=18.6326, with dimensions x=56.7368, y=75.1330, z=65.4370. For α-amylase, the center coordinates were x=8.4474, y=27.9862, z=49.1350, with dimensions x=58.9736, y=73.7796, z=58.5527. The molecular interactions were visualized using Biovia Discovery Studio 2019, which provided a graphical representation of the chemical interactions and displayed both 3D and 2D images. The optimal interaction was determined by evaluating the binding energy, measured in kcal/mol (38).

3. Results and Discussion

3.1. Phytochemical Compounds Identification

Plants containing phytochemical substances have been utilized in the treatment of various significant health issues, including mangrove. *A. ilicifolius* has been extensively utilized as a traditional remedy in India and China due to the presence of phytochemical components in this botanical species. The phytochemical screening revealed the presence of glycoside, alkaloid, flavonoid, triterpenoid, steroid, fatty acid, and saponin in *A. ilicifolius* (39). Phytochemical compounds of *A. ilicifolius* were identified by LC-HRMS (Table 1).

The phytochemical components of *A. ilicifolius*, a type of mangrove plant, were extracted using the step maceration extraction method and tentatively identified using LC-HRMS analysis. The ethyl acetate extract contains five known compounds: apigenin, glycitein, 4-coumaric acid, oleanolic acid, and reserpine. Table 1 indicates that the methanol extract derived from *A. ilicifolius* leaves included the following compounds: flurandrenolide, corymboside, scutellarin, apigenin 7-O-glucuronide, luteolin, glycitein, and reserpine. Glycitein and reserpine have been detected in both the ethyl acetate and methanol extracts, exhibiting comparable retention times.

Table 1. Phytochemical compounds identified tentatively from *A. ilicifolius.*

RT (min)	Molecular weight	Formula	Compound name	m/z cloudbest match
Methanol Extract				
0.904	462.0801	$C_{24}H_{33}FO_6$	Flurandrenolide	93
6.287	564.1483	$C_{26}H_{28}O_{14}$	Corymboside	91.6
7.363	462.0801	$C_{21}H_{18}O_{12}$	Scutellarin	98.3
8.116	446.0852	$C_{21}H_{18}O_{11}$	Apigenin 7-O-glucuronide	98.2
9.792	286.0475	$C_{15}H_{10}O_6$	Luteolin	99.4
13.664	284.0684	$C_{16}H_{12}O_5$	Glycitein	98.4
20.937	608.2637	$C_{33}H_{40}N_2O_9$	Reserpine	81
Ethyl acetate Extract				
10.924	270.0528	$C_{15}H_{10}O_5$	Apigenin	99.5
13.669	284.0684	$C_{16}H_{12}O_5$	Glycitein	98.5
18.935	164.0470	$C_9H_8O_3$	4-Coumaric acid	98.1
20.705	438.3496	$C_{30}H_{48}O_3$	Oleanolic acid	94.5
20.710	608.2625	$C_{33}H_{40}N_2O_9$	Reserpine	83.3

RT = retention time, m/z = mass to charge ratio

Table 1 categorizes the phytoconstituents found in *A. ilicifolius* into four groups: steroids (flurandrenolide), terpenoids (oleanolic acid), alkaloids (reserpine), and flavonoids (corymboside, scutellarin, apigenin 7-O-glucuronide, luteolin, glycitein, apigenin, 4-coumaric acid). Flurandrenolide, a steroid chemical, is derived from the leaves of *Peltophorum pterocarpum* (40) and the rhizome extract of Curcuma zedoaria (41). Reserpine, a primary constituent of the roots of *Rauwolfia serpentina*, is a terpene indole alkaloid that has been extensively employed for the treatment of hypertension(42–44). Oleanolic acid, a terpenoid, was extracted from *Cuscuta reflexa, Sonneratia caseolaris* fruits, and *Sonneratia alba* mangrove leaves (15). Corymboside was classified as di-*C*-glycosyflavone, and isolated for the first time from *Carlina corymbose* root (45). Scutellarin is a key flavonoid found in the traditional Chinese medicines *Erigon breviscapus* (46), *E. multiradiatus* (47), and it was isolated from *Scutellaria barbata* (48). Flavonoids have many pharmacological effects, including their ability to act as antidiabetic agents. The herbal remedy TOTUM63 was found to include luteolin, apigenin, and apigenin-7-O-glucuronide. Consumption of this medicine

was reported to be effective in preventing fluctuating hyperglycemia (49). Flavonoids are considered to be the active molecules in nutritional and herbal materials.

3.2. Molecular Docking

Molecular docking research was conducted on ligands observed using LC-HRMS to determine their binding affinity and elucidate the manner that justifies their inhibitory effect. The binding affinity between chemicals isolated from *A. ilicifolius* leaves, acting as ligands, and the α-glucosidase receptor (PDB ID: 3A4A) was determined to range from -6.7 to -10 kcal/mol (Table 2). The binding affinities of the molecular docking between the ligands miglitol, voglibose, and acarbose, and the receptor were -6.0, -6.1, and -8.1 kcal/mol, respectively. The chemical with the most binding affinity to the receptor among those found in the extract of *A. ilicifolius* leaves was reserpine, with a binding energy of -10 kcal/mol. On the other hand, the chemical interaction between 4-coumaric acid and the receptor had the lowest binding affinity, measuring -6.7 kcal/mol. The binding affinity of scuttelarin and apigenin-7-O-glucoronide was -9.9 kcal/mol, which is nearly equivalent to the binding energy of reserpine. The binding affinity value between the receptor and the chemicals found in the *A. ilicifolius* extract was lower than that between the receptor and the ligand control (-5.9 kcal/mol). The decreased binding affinity between the receptor and ligands resulted in increased inhibitory enzyme activity (50). According to this study, the alkaloid and flavonoid had a higher binding affinity compared to common medications like acarbose, miglitol, and voglibose. The binding affinity between the receptor and the discovered compounds of *A. ilicifolius* was higher, ranging from -8.2 to -10 kcal/mol, compared to the binding affinity of the commercial drugs, which included acarbose (-8.1 kcal/mol), miglitol (-5.2 kcal/mol), voglibose (-6.1 kcal/mol), and the receptor itself. Furthermore, the binding affinity between the receptor and p-coumaric acid was determined to be -6.7 kcal/mol, which was found to be greater than the binding affinity of miglitol (-5.2 kcal/mol) and voglibose (-6.1 kcal/mol). The study found that the complex ligands, including reserpine, scuttelarin, and apigenin-7-glucoronide, exhibited the highest binding affinity value in molecular docking with the receptor (51).

Table 2. Molecular docking analysis of phytochemical compounds identified tentatively from *A. ilicifolius* with receptor α-glucosidase and α-amylase

Compounds	Binding Affinity (α-glucosidase)	Binding Affinity (α-amylase)
Acarbose	-8.1	-8.3
Miglitol	-6	-5.2
Voglibose	-6.1	-6.4
Reserpine	-10	-8.6
Oleanolic acid	-8.6	-9.3
4 Coumaric acid	-6.7	-6.1
Apigenin	-8.6	-8.2
Glycitein	-8.2	-7.9
Flurandrenolide	-8.3	-8.4
Scutellarin	-9.9	-9
Apigenin-7-O-glucuronide	-9.9	-9.1
Corymboside	-9.3	-9.3
GLC	-5.9	-
NAG	-	-5.7
MYC	-	-7.9

The enzyme isomaltase *Saccharomyces cereviceae* is comprised of 589 amino acids, which are organized into three distinct domains. Domain A consists of residues 1-113 and 190-512, with catalytic residues Asp215, Glu277, and Asp352 located on the C-terminal. Domain B contains residues 114-189. Domain C spans residues 518-589 (52). The presence of a catalytic residue suggests that the active site of the protein enzyme, as well as all the residues involved in the molecular interaction with 3A4A, have played a role in the actual catalytic reaction (51). Figures 1-illustrate the 3D and 2D visualization of the molecular interaction between α-glucosidase and ligand.With regards to the visualization, all of the compounds were bound to domain A, where the catalytic residue is found. The predicted inhibitory mechanisms of the ligands from *A. ilicifolius* extract were found to be similar to those of ligands control and ligands from known substances (51).

Table 3 presented the molecular interaction between α-glucosidase and the native, control, and identified components of the *A. ilicifolius* extract. In addition to hydrogen bonding, various types of non-covalent bonds have been identified, including Pi-Cation, Pi-Anion, Pi-Pi T shaped, and Pi-Pi alkyl interactions. Reserpine, scuttelarin, and apigenin-7-glucuronide exhibited greater binding affinity in comparison to other interactions. The high binding affinity is attributed to the chemical structure present in these compounds, which consist of three types: aromatic, alicyclic, and aliphatic. There was a potential for those chemicals to interact with three catalytic residues, namely Asp215, Glu277, and Asp352 (51). Reserpine formed an electrostatic connection with the catalytic residue Asp352 through Pi-cation interaction. Scuttellarin exhibits electrostatic binding with Asp352 and hydrogen bonding with Asp215. In addition, apigenin-7-glucuronide formed an electrostatic link with Asp352, as well as a Pi-Anion interaction and a hydrogen bond with Asp215. Glycitein and Corymboside formed hydrogen bonds with Glu277, among other molecules. The catalytic reaction in digestion enzymes and ligands is influenced by the number and distance of hydrogen bonds, which in turn leads to variations in the inhibitory activity of digestion enzymes (53). Ligands was stabilized on the binding location by Van der Waals and non-polar energy (54).

Table 3. Molecular interaction between ligand and α-glucosidase (PDB ID : 3A4A) and α-amylase (PDB ID : 4GQR).

Ligand	Interaction	Distance (Å)	Category	Type
α-Glucosidase (PDB ID : 3A4A)				
Acarbose	A:SER298:HG - N:UNK1:O	2.14375	Hydrogen Bond	Conventional Hydrogen Bond
	N:UNK1:H - A:ARG263:O	2.36568	Hydrogen Bond	Conventional Hydrogen Bond
	N:UNK1:H - A:VAL266:O	1.88316	Hydrogen Bond	Conventional Hydrogen Bond
	N:UNK1:H - N:UNK1:O	2.0231	Hydrogen Bond	Conventional Hydrogen Bond
	N:UNK1:H - A:ASN264:O	2.60763	Hydrogen Bond	Conventional Hydrogen Bond
	N:UNK1:H - A:ASN264:O	2.74108	Hydrogen Bond	Conventional Hydrogen Bond
	N:UNK1:H - A:ARG263:O	2.43567	Hydrogen Bond	Conventional Hydrogen Bond
	N:UNK1:H - N:UNK1:O	2.28203	Hydrogen Bond	Conventional Hydrogen Bond

Ligand	Interaction	Distance (Å)	Category	Type
	N:UNK1:H - A:ILE272:O	2.67779	Hydrogen Bond	Conventional Hydrogen Bond
	N:UNK1:H - A:ASN259:OD1	2.68057	Hydrogen Bond	Conventional Hydrogen Bond
	N:UNK1:H - A:ALA292:O	2.27231	Hydrogen Bond	Conventional Hydrogen Bond
Miglitol	N:UNK1:C - A:GLU422:OE2	3.41299	Hydrogen Bond	Carbon Hydrogen Bond
	N:UNK1:C - A:HIS423:NE2	3.14841	Hydrogen Bond	Carbon Hydrogen Bond
Voglibose	A:GLU296:HN - N:UNK1:O	2.51541	Hydrogen Bond	Conventional Hydrogen Bond
	N:UNK1:H - A:ASN259:OD1	2.73475	Hydrogen Bond	Conventional Hydrogen Bond
	N:UNK1:H - N:UNK1:O	1.90859	Hydrogen Bond	Conventional Hydrogen Bond
	N:UNK1:H - A:GLU296:O	2.34397	Hydrogen Bond	Conventional Hydrogen Bond
	N:UNK1:H - N:UNK1:N	2.31984	Hydrogen Bond	Conventional Hydrogen Bond
	N:UNK1:H - A:GLU296:O	3.03279	Hydrogen Bond	Conventional Hydrogen Bond
	A:ALA292:CA - N:UNK1:O	3.71454	Hydrogen Bond	Carbon Hydrogen Bond
	N:UNK1:C - A:ILE272:O	3.39589	Hydrogen Bond	Carbon Hydrogen Bond
	N:UNK1:C - A:ILE272:O	3.5493	Hydrogen Bond	Carbon Hydrogen Bond
	N:UNK1:C - A:ASN259:OD1	3.02085	Hydrogen Bond	Carbon Hydrogen Bond
	N:UNK1:C - A:ALA292:O	3.29531	Hydrogen Bond	Carbon Hydrogen Bond
Reserpine	N:UNK1:C - A:ASP69:OD2	3.54448	Hydrogen Bond	Carbon Hydrogen Bond
	A:ARG442:NH1 - N:UNK1	3.49675	Hydrogen Bond	Carbon Hydrogen Bond
	A:ASP307:OD2 - N:UNK1	3.54382	Hydrogen Bond	Carbon Hydrogen Bond
	A:ASP352:OD1 - N:UNK1	3.68006	Electrostatic	Pi-Cation
	N:UNK1:C - A:HIS280	3.53364	Electrostatic	Pi-Anion
	A:ARG315 - N:UNK1	4.86026	Electrostatic	Pi-Anion
	A:ARG315 - N:UNK1	3.70585	Hydrophobic	Pi-Sigma
	A:PHE303 - N:UNK1	4.9761	Hydrophobic	Alkyl
	N:UNK1 - A:PRO312	4.8296	Hydrophobic	Alkyl
	N:UNK1:C - A:ASP69:OD2	4.94677	Hydrophobic	Pi-Alkyl
	A:ARG442:NH1 - N:UNK1	4.53006	Hydrophobic	Pi-Alkyl
Oleanolic acid	A:LYS148 - N:UNK1	4.77619	Hydrophobic	Alkyl
	A:PRO149 - N:UNK1	4.70546	Hydrophobic	Alkyl
	A:ALA418 - N:UNK1:C	4.03383	Hydrophobic	Alkyl
	N:UNK1:C - A:LYS148	3.76716	Hydrophobic	Alkyl

Ligand	Interaction	Distance (Å)	Category	Type
	N:UNK1:C - A:PRO149	5.12883	Hydrophobic	Alkyl
	N:UNK1:C - A:PRO149	4.24092	Hydrophobic	Alkyl
	A:PHE166 - N:UNK1:C	5.1307	Hydrophobic	Pi-Alkyl
4-coumaric acid	A:GLY161:HN - N:UNK1:O	2.37645	Hydrogen Bond	Conventional Hydrogen Bond
	N:UNK1:H - A:GLU422:OE1	1.93763	Hydrogen Bond	Conventional Hydrogen Bond
	A:GLY160:CA - N:UNK1:O	3.73675	Hydrogen Bond	Carbon Hydrogen Bond
	A:HIS423 - N:UNK1	5.17559	Hydrophobic	Pi-Pi T-shaped
	N:UNK1 - A:ILE419	5.15365	Hydrophobic	Pi-Alkyl
Apigenin	A:THR274:HG1 - N:UNK1:O	2.94767	Hydrogen Bond	Conventional Hydrogen Bond
	A:THR274:HG1 - N:UNK1:O	2.13893	Hydrogen Bond	Conventional Hydrogen Bond
	N:UNK1:H - A:ARG263:O	2.40239	Hydrogen Bond	Conventional Hydrogen Bond
	N:UNK1:H - A:GLU296:O	2.19953	Hydrogen Bond	Conventional Hydrogen Bond
	N:UNK1 - A:ARG263	3.93928	Hydrophobic	Pi-Alkyl
	N:UNK1 - A:VAL266	4.90905	Hydrophobic	Pi-Alkyl
Glycitein	A:ARG442:HH11 - N:UNK1:O	2.54096	Hydrogen Bond	Conventional Hydrogen Bond
	N:UNK1:H - A:GLU277:OE2	1.9746	Hydrogen Bond	Conventional Hydrogen Bond
	A:GLU411:OE2 - N:UNK1	4.21302	Electrostatic	Pi-Anion
	A:TYR158 - N:UNK1	5.5587	Hydrophobic	Pi-Pi T-shaped
	N:UNK1 - A:ARG315	5.09293	Hydrophobic	Pi-Alkyl
Flurandrenolide	A:ARG176:HH12 - N:UNK1:O	1.81296	Hydrogen Bond	Conventional Hydrogen Bond
	A:ARG176:HH22 - N:UNK1:O	2.81358	Hydrogen Bond	Conventional Hydrogen Bond
	N:UNK1:H - A:GLY160:O	2.36531	Hydrogen Bond	Conventional Hydrogen Bond
	N:UNK1:H - A:GLU421:OE2	2.07513	Hydrogen Bond	Conventional Hydrogen Bond
	A:TRP164:O - N:UNK1:F	3.66097	Halogen	Halogen (Fluorine)
	A:PRO151 - N:UNK1	5.49852	Hydrophobic	Alkyl
	A:TRP238 - N:UNK1:C	5.09977	Hydrophobic	Pi-Alkyl
Scuttelarin	N:UNK1:H - A:SER240:OG	2.74095	Hydrogen Bond	Conventional Hydrogen Bond
	N:UNK1:H - A:ASP242:OD2	2.76077	Hydrogen Bond	Conventional Hydrogen Bond
	N:UNK1:H - A:ASP215:OD1	2.75749	Hydrogen Bond	Conventional Hydrogen Bond
	N:UNK1:H - A:ASP215:OD2	2.77638	Hydrogen Bond	Conventional Hydrogen Bond
	A:ASP352:OD2 - N:UNK1	4.27256	Electrostatic	Pi-Anion
	N:UNK1 - A:VAL216	5.10967	Hydrophobic	Pi-Alkyl

Ligand	Interaction	Distance (Å)	Category	Type
Apigenin-7-glucoronide	N:UNK1:H - A:SER240:OG	2.34823	Hydrogen Bond	Conventional Hydrogen Bond
	N:UNK1:H - A:ASP242:OD2	2.1196	Hydrogen Bond	Conventional Hydrogen Bond
	N:UNK1:H - A:ASP215:OD2	2.25959	Hydrogen Bond	Conventional Hydrogen Bond
	A:TYR158:CA - N:UNK1:O	3.58838	Hydrogen Bond	Carbon Hydrogen Bond
	A:ARG442:NH1 - N:UNK1	4.87541	Electrostatic	Pi-Cation
	A:ASP352:OD2 - N:UNK1	4.68838	Electrostatic	Pi-Anion
	A:GLU411:OE2 - N:UNK1	4.83346	Electrostatic	Pi-Anion
	A:PHE303 - N:UNK1	5.55452	Hydrophobic	Pi-Pi Stacked
	A:PHE303 - N:UNK1	5.91265	Hydrophobic	Pi-Pi Stacked
	N:UNK1 - A:VAL216	5.02374	Hydrophobic	Pi-Alkyl
Corymboside	N:UNK1:H - A:SER311:O	2.15572	Hydrogen Bond	Conventional Hydrogen Bond
	N:UNK1:H - A:THR310:OG1	2.72685	Hydrogen Bond	Conventional Hydrogen Bond
	N:UNK1:H - A:ASP307:OD1	2.38367	Hydrogen Bond	Conventional Hydrogen Bond
	N:UNK1:H - A:ASP352:O	2.51825	Hydrogen Bond	Conventional Hydrogen Bond
	N:UNK1:H - A:GLU277:OE2	2.81656	Hydrogen Bond	Conventional Hydrogen Bond
	N:UNK1:C - A:ASP307:OD2	3.79187	Hydrogen Bond	Carbon Hydrogen Bond
GLC	A:THR274:HG1 - N:UNK1:O	2.30523	Hydrogen Bond	Conventional Hydrogen Bond
	A:HIS295:HD1 - N:UNK1:O	2.04856	Hydrogen Bond	Conventional Hydrogen Bond
	N:UNK1:H - A:LEU297:O	1.89985	Hydrogen Bond	Conventional Hydrogen Bond
	N:UNK1:H - A:GLU296:O	2.5219	Hydrogen Bond	Conventional Hydrogen Bond
	N:UNK1:H - A:ASN259:OD1	1.97831	Hydrogen Bond	Conventional Hydrogen Bond
	N:UNK1:C - A:ILE272:O	3.6925	Hydrogen Bond	Carbon Hydrogen Bond
α-Amylase (PDB ID : 4GQR)				
Acarbose	A:SER289:OG - N:UNK1:O	3.01693	Hydrogen Bond	Conventional Hydrogen Bond
	A:GLY334:N - N:UNK1:O	3.25458	Hydrogen Bond	Conventional Hydrogen Bond
	A:GLY403:N - N:UNK1:O	2.97658	Hydrogen Bond	Conventional Hydrogen Bond
	N:UNK1:H - N:UNK1:O	2.2388	Hydrogen Bond	Conventional Hydrogen Bond

Ligand	Interaction	Distance (Å)	Category	Type
	N:UNK1:H - A:TRP280:O	1.91551	Hydrogen Bond	Conventional Hydrogen Bond
	N:UNK1:H - A:GLU282:OE2	2.92862	Hydrogen Bond	Conventional Hydrogen Bond
	N:UNK1:H - A:GLN404:O	2.05277	Hydrogen Bond	Conventional Hydrogen Bond
	N:UNK1:H - N:UNK1:O	2.40391	Hydrogen Bond	Conventional Hydrogen Bond
	N:UNK1:H - N:UNK1:O	2.21434	Hydrogen Bond	Conventional Hydrogen Bond
	N:UNK1:H - A:ASP402:OD1	2.40917	Hydrogen Bond	Conventional Hydrogen Bond
	N:UNK1:H - A:ASP402:OD1	2.65188	Hydrogen Bond	Conventional Hydrogen Bond
	N:UNK1:H - N:UNK1:O	2.38548	Hydrogen Bond	Conventional Hydrogen Bond
	N:UNK1:C - A:HIS331:NE2	3.73739	Hydrogen Bond	Carbon Hydrogen Bond
	N:UNK1:C - A:PRO332:O	3.64756	Hydrogen Bond	Carbon Hydrogen Bond
Miglitol	N:UNK1:H - A:SER289:OG	2.70624	Hydrogen Bond	Conventional Hydrogen Bond
	N:UNK1:C - A:GLY334:O	3.50221	Hydrogen Bond	Carbon Hydrogen Bond
	N:UNK1:C - A:PRO332:O	3.41058	Hydrogen Bond	Carbon Hydrogen Bond
	N:UNK1:C - A:PRO332:O	3.59053	Hydrogen Bond	Carbon Hydrogen Bond
	N:UNK1:C - A:GLY334:O	3.6633	Hydrogen Bond	Carbon Hydrogen Bond
Voglibose	A:ARG398:NE - N:UNK1:O	3.12962	Hydrogen Bond	Conventional Hydrogen Bond
	A:ARG421:NH2 - N:UNK1:O	2.8173	Hydrogen Bond	Conventional Hydrogen Bond
	N:UNK1:H - A:SER289:OG	2.43068	Hydrogen Bond	Conventional Hydrogen Bond
	N:UNK1:H - A:GLY334:O	2.35555	Hydrogen Bond	Conventional Hydrogen Bond
	N:UNK1:H - A:ASP402:OD1	2.87956	Hydrogen Bond	Conventional Hydrogen Bond
	A:PHE335:CA - N:UNK1:O	3.72306	Hydrogen Bond	Carbon Hydrogen Bond
Reserpine	A:LYS200:NZ - N:UNK1:O	2.9711	Hydrogen Bond	Conventional Hydrogen Bond
	N:UNK1:C - A:ASP300:OD2	3.57468	Hydrogen Bond	Carbon Hydrogen Bond
	N:UNK1:C - A:HIS101:NE2	3.66247	Hydrogen Bond	Carbon Hydrogen Bond
	N:UNK1:C - A:ASP197:OD2	3.61969	Hydrogen Bond	Carbon Hydrogen Bond
	A:TYR151:OH - N:UNK1	4.16455	Hydrogen Bond	Pi-Donor Hydrogen Bond
	A:TRP59 - N:UNK1	3.7075	Hydrophobic	Pi-Pi Stacked

Ligand	Interaction	Distance (Å)	Category	Type
	A:TRP59 - N:UNK1	4.35563	Hydrophobic	Pi-Pi Stacked
	A:TYR151 - N:UNK1	4.96103	Hydrophobic	Pi-Pi Stacked
	A:LEU162 - N:UNK1	4.41577	Hydrophobic	Alkyl
	N:UNK1 - A:LEU162	5.18016	Hydrophobic	Alkyl
	N:UNK1 - A:ILE235	5.34773	Hydrophobic	Pi-Alkyl
Oleanolic acid	A:ARG195:NH2 - N:UNK1:O	3.10673	Hydrogen Bond	Conventional Hydrogen Bond
	N:UNK1:H - A:ASP197:OD1	2.38095	Hydrogen Bond	Conventional Hydrogen Bond
	N:UNK1:H - A:GLU233:OE1	2.46475	Hydrogen Bond	Conventional Hydrogen Bond
	A:LEU162 - N:UNK1	5.15117	Hydrophobic	Alkyl
	A:ALA198 - N:UNK1:C	3.85911	Hydrophobic	Alkyl
	N:UNK1:C - A:LEU165	5.01917	Hydrophobic	Alkyl
	N:UNK1:C - A:LEU162	5.41201	Hydrophobic	Alkyl
	A:TRP58 - N:UNK1:C	4.84643	Hydrophobic	Pi-Alkyl
	A:TRP59 - N:UNK1	5.49293	Hydrophobic	Pi-Alkyl
	A:TRP59 - N:UNK1	5.49177	Hydrophobic	Pi-Alkyl
	A:TRP59 - N:UNK1:C	4.21936	Hydrophobic	Pi-Alkyl
	A:TRP59 - N:UNK1:C	4.36492	Hydrophobic	Pi-Alkyl
	A:TYR62 - N:UNK1:C	4.54531	Hydrophobic	Pi-Alkyl
	A:TYR62 - N:UNK1:C	5.17048	Hydrophobic	Pi-Alkyl
	A:HIS305 - N:UNK1:C	4.5606	Hydrophobic	Pi-Alkyl
4-Coumaric acid	N:UNK1:H - A:ASP197:OD1	2.56274	Hydrogen Bond	Conventional Hydrogen Bond
	A:TYR62 - N:UNK1	4.41847	Hydrophobic	Pi-Pi Stacked
Apigenin	N:UNK1:H - A:ASP197:OD1	2.13971	Hydrogen Bond	Conventional Hydrogen Bond
	N:UNK1:H - A:GLU233:OE1	2.69221	Hydrogen Bond	Conventional Hydrogen Bond
	N:UNK1:H - A:GLN63:OE1	2.80652	Hydrogen Bond	Conventional Hydrogen Bond
	N:UNK1:H - N:UNK1:O	2.54813	Hydrogen Bond	Conventional Hydrogen Bond
	A:ASP300:OD2 - N:UNK1	4.66716	Electrostatic	Pi-Anion
	A:TRP59 - N:UNK1	5.37905	Hydrophobic	Pi-Pi Stacked
	A:TRP59 - N:UNK1	3.96057	Hydrophobic	Pi-Pi Stacked
	A:TRP59 - N:UNK1	4.38645	Hydrophobic	Pi-Pi Stacked
	A:TYR62 - N:UNK1	4.67074	Hydrophobic	Pi-Pi Stacked
Glycitein	N:UNK1:H - A:HIS299:NE2	2.79747	Hydrogen Bond	Conventional Hydrogen Bond
	A:ASP197:OD1 - N:UNK1	4.54317	Electrostatic	Pi-Anion
	A:ASP300:OD2 - N:UNK1	3.81865	Electrostatic	Pi-Anion
	N:UNK1:C - A:TRP59	3.70491	Hydrophobic	Pi-Sigma
	A:TRP59 - N:UNK1	4.72881	Hydrophobic	Pi-Pi Stacked
	A:TRP59 - N:UNK1	4.86053	Hydrophobic	Pi-Pi Stacked
	A:TYR62 - N:UNK1	4.98133	Hydrophobic	Pi-Pi T-shaped
Flurandrenolide	N:UNK1:H - A:ASP197:OD2	2.82938	Hydrogen Bond	Conventional Hydrogen Bond
	N:UNK1:C - A:TRP59	3.68192	Hydrophobic	Pi-Sigma

Ligand	Interaction	Distance (Å)	Category	Type
	N:UNK1:C - A:TRP59	3.91273	Hydrophobic	Pi-Sigma
	A:TRP58 - N:UNK1	4.54605	Hydrophobic	Pi-Alkyl
	A:TRP59 - N:UNK1	5.05187	Hydrophobic	Pi-Alkyl
	A:TRP59 - N:UNK1	5.43755	Hydrophobic	Pi-Alkyl
	A:TRP59 - N:UNK1	4.40163	Hydrophobic	Pi-Alkyl
	A:TRP59 - N:UNK1:C	5.07744	Hydrophobic	Pi-Alkyl
Scuttelarin	N:UNK1:H - A:GLU233:OE2	2.8829	Hydrogen Bond	Conventional Hydrogen Bond
	N:UNK1:H - N:UNK1:O	2.04561	Hydrogen Bond	Conventional Hydrogen Bond
	N:UNK1:H - A:ASP197:OD1	1.8651	Hydrogen Bond	Conventional Hydrogen Bond
	N:UNK1:H - A:ASP197:OD2	2.41018	Hydrogen Bond	Conventional Hydrogen Bond
	N:UNK1:H - A:TYR62:O	3.03797	Hydrogen Bond	Conventional Hydrogen Bond
	N:UNK1:H - N:UNK1:O	2.76402	Hydrogen Bond	Conventional Hydrogen Bond
	A:TRP59 - N:UNK1	3.84166	Hydrophobic	Pi-Pi Stacked
	A:TRP59 - N:UNK1	5.17217	Hydrophobic	Pi-Pi Stacked
	A:TRP59 - N:UNK1	4.42315	Hydrophobic	Pi-Pi Stacked
	A:TRP59 - N:UNK1	4.17295	Hydrophobic	Pi-Pi Stacked
	A:TRP59 - N:UNK1	5.15709	Hydrophobic	Pi-Pi Stacked
Apigenin-7-glucuronide	N:UNK1:H - A:ASP300:OD1	2.72062	Hydrogen Bond	Conventional Hydrogen Bond
	N:UNK1:H - A:GLU233:OE1	2.52251	Hydrogen Bond	Conventional Hydrogen Bond
	N:UNK1:H - A:GLU233:OE2	2.50855	Hydrogen Bond	Conventional Hydrogen Bond
	N:UNK1:H - A:ASP197:OD1	1.82764	Hydrogen Bond	Conventional Hydrogen Bond
	N:UNK1:H - A:ASP197:OD2	2.76806	Hydrogen Bond	Conventional Hydrogen Bond
	A:TRP59 - N:UNK1	3.86822	Hydrophobic	Pi-Pi Stacked
	A:TRP59 - N:UNK1	5.19079	Hydrophobic	Pi-Pi Stacked
	A:TRP59 - N:UNK1	4.45411	Hydrophobic	Pi-Pi Stacked
	A:TRP59 - N:UNK1	4.17154	Hydrophobic	Pi-Pi Stacked
	A:TRP59 - N:UNK1	5.18598	Hydrophobic	Pi-Pi Stacked
Corymboside	A:CYS378:N - N:UNK1:O	2.98229	Hydrogen Bond	Conventional Hydrogen Bond
	A:GLN390:NE2 - N:UNK1:O	2.97841	Hydrogen Bond	Conventional Hydrogen Bond
	N:UNK1:H - A:TRP382:O	2.40885	Hydrogen Bond	Conventional Hydrogen Bond
	N:UNK1:H - A:VAL383:O	1.96561	Hydrogen Bond	Conventional Hydrogen Bond
	N:UNK1:H - A:CYS378:O	2.05586	Hydrogen Bond	Conventional Hydrogen Bond
	A:TRP316:CA - N:UNK1:O	3.58121	Hydrogen Bond	Carbon Hydrogen Bond
	A:ARG389:N - N:UNK1	4.11813	Hydrogen Bond	Pi-Donor Hydrogen Bond
	A:TRP388 - N:UNK1	3.84491	Hydrophobic	Pi-Pi Stacked

Ligand	Interaction	Distance (Å)	Category	Type
	A:TRP388 - N:UNK1	3.98672	Hydrophobic	Pi-Pi Stacked
	A:TRP388 - N:UNK1	4.80253	Hydrophobic	Pi-Pi Stacked
	A:TRP388 - N:UNK1	4.24323	Hydrophobic	Pi-Pi Stacked
NAG	N:UNK1:H - N:UNK1:O	2.83821	Hydrogen Bond	Conventional Hydrogen Bond
	N:UNK1:H - N:UNK1:O	2.09734	Hydrogen Bond	Conventional Hydrogen Bond
	N:UNK1:H - A:ASP197:OD1	2.15724	Hydrogen Bond	Conventional Hydrogen Bond
	N:UNK1:H - A:GLU233:OE1	2.85765	Hydrogen Bond	Conventional Hydrogen Bond
MYC	A:SER3:OG - N:UNK1:O	2.93106	Hydrogen Bond	Conventional Hydrogen Bond
	A:THR6:OG1 - N:UNK1:O	2.72914	Hydrogen Bond	Conventional Hydrogen Bond
	N:UNK1:H - A:PRO332:O	2.92417	Hydrogen Bond	Conventional Hydrogen Bond
	N:UNK1:H - A:THR6:O	2.23603	Hydrogen Bond	Conventional Hydrogen Bond
	N:UNK1:H - N:UNK1:O	2.27477	Hydrogen Bond	Conventional Hydrogen Bond
	N:UNK1 - A:PRO4	4.68308	Hydrophobic	Pi-Alkyl
	N:UNK1 - A:PRO4	3.98943	Hydrophobic	Pi-Alkyl

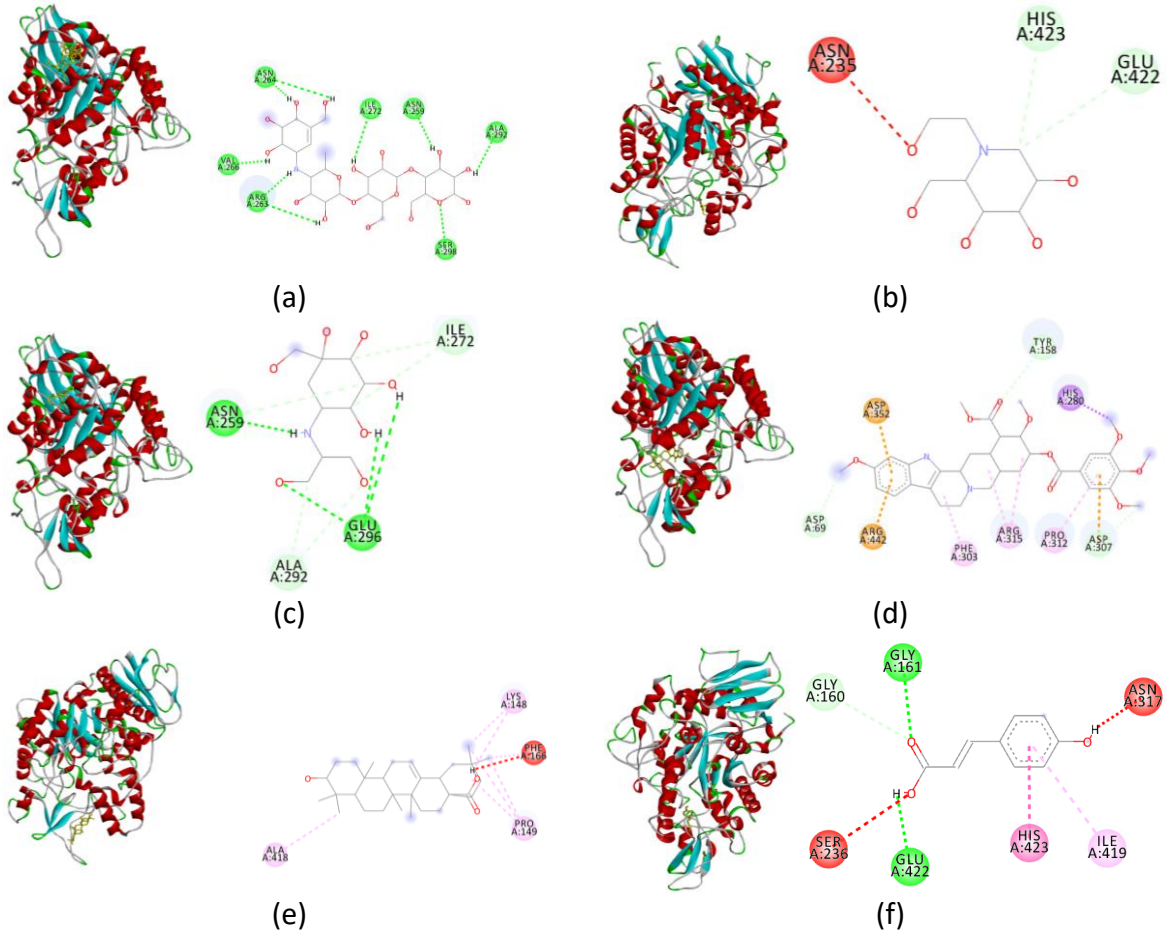

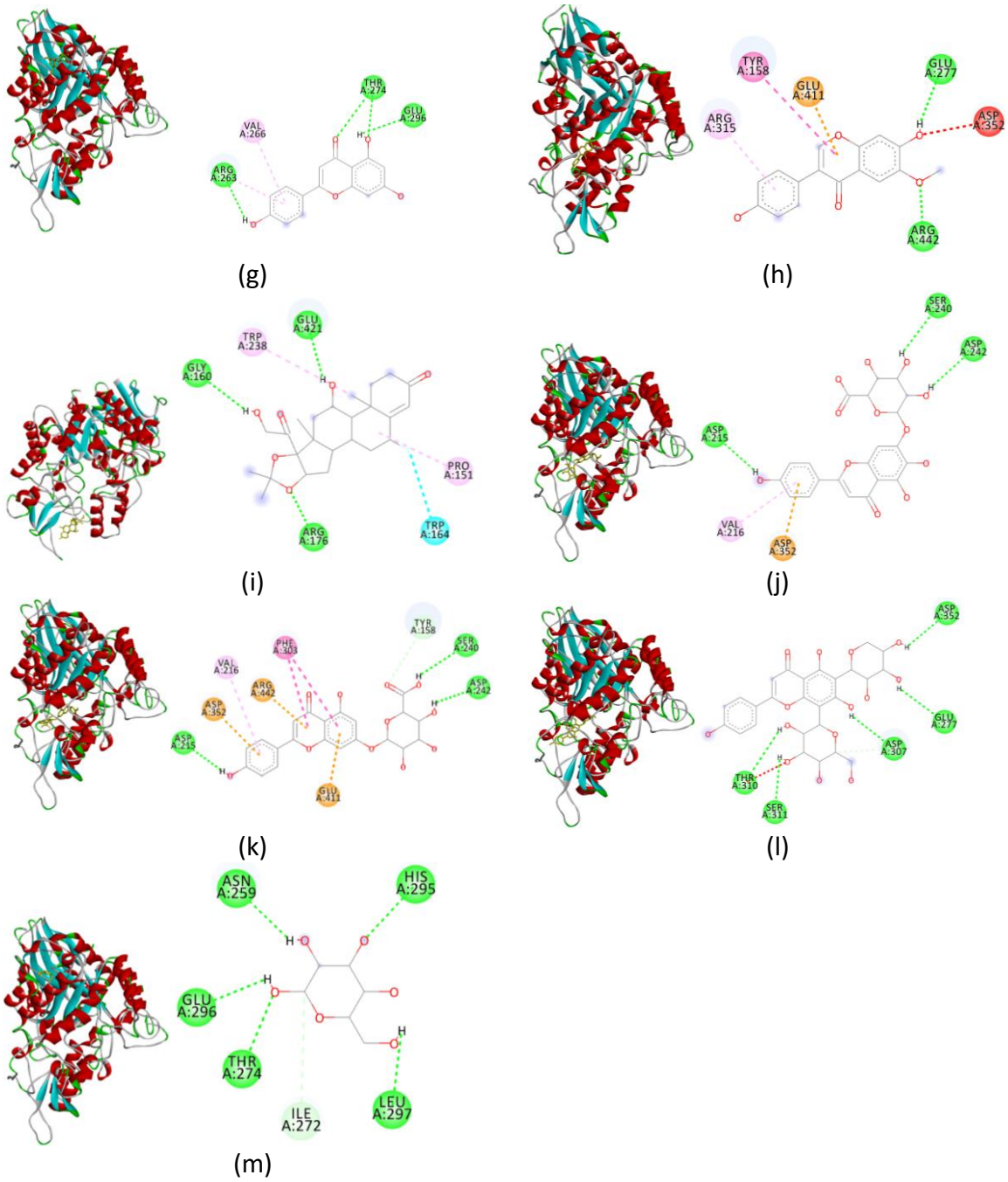

Figure 1. Visualization 3D (a) and 2D (b) binding interaction of α-glucosidase (3A4A) with acarbose(a), miglitol(b), voglibose(c), reserpine(d), oleanolic acid(e), coumaric acid(f), apigenin(g), glycitein(h), flurandrenolide(i), scuttelarin(j), apigenin-7-*O*-glucoronide(k), corymboside(l), and GLC(m).

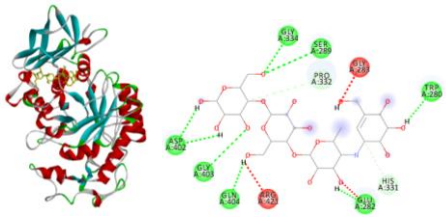

(a)

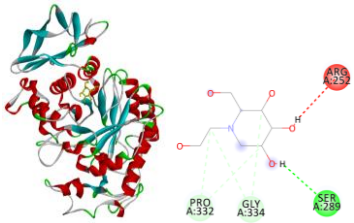

(b)

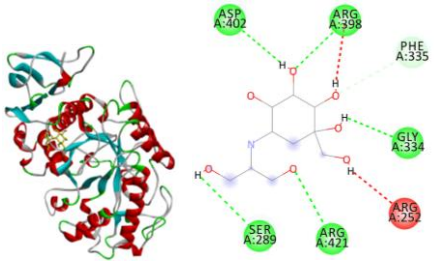

(c)

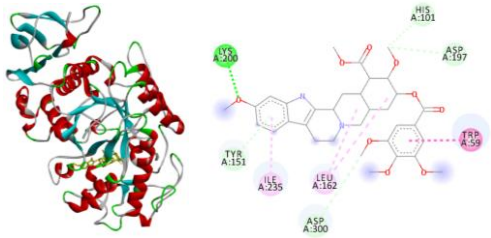

(d)

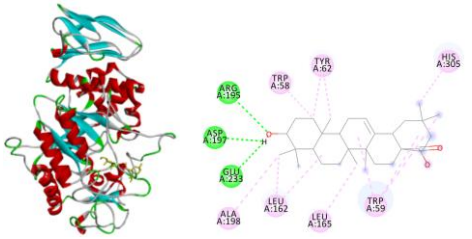

(e)

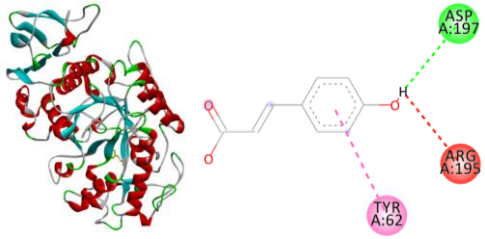

(f)

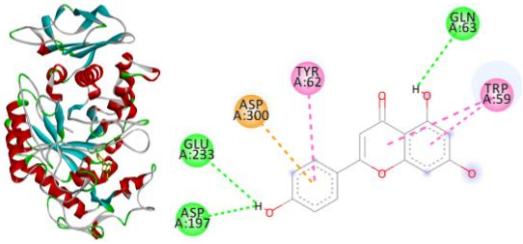

(g)

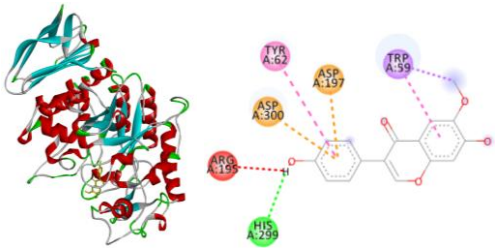

(h)

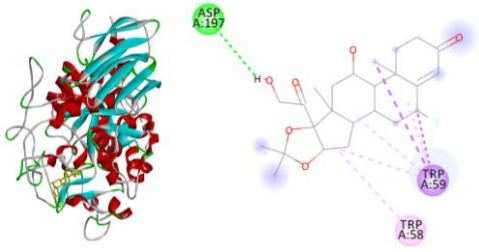

(i)

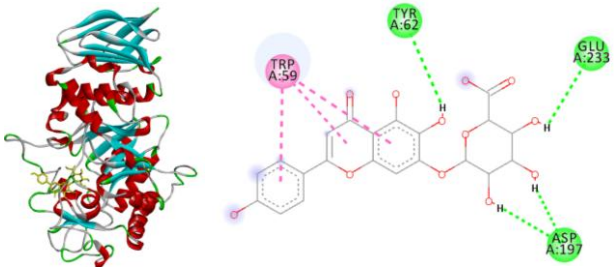

(j)

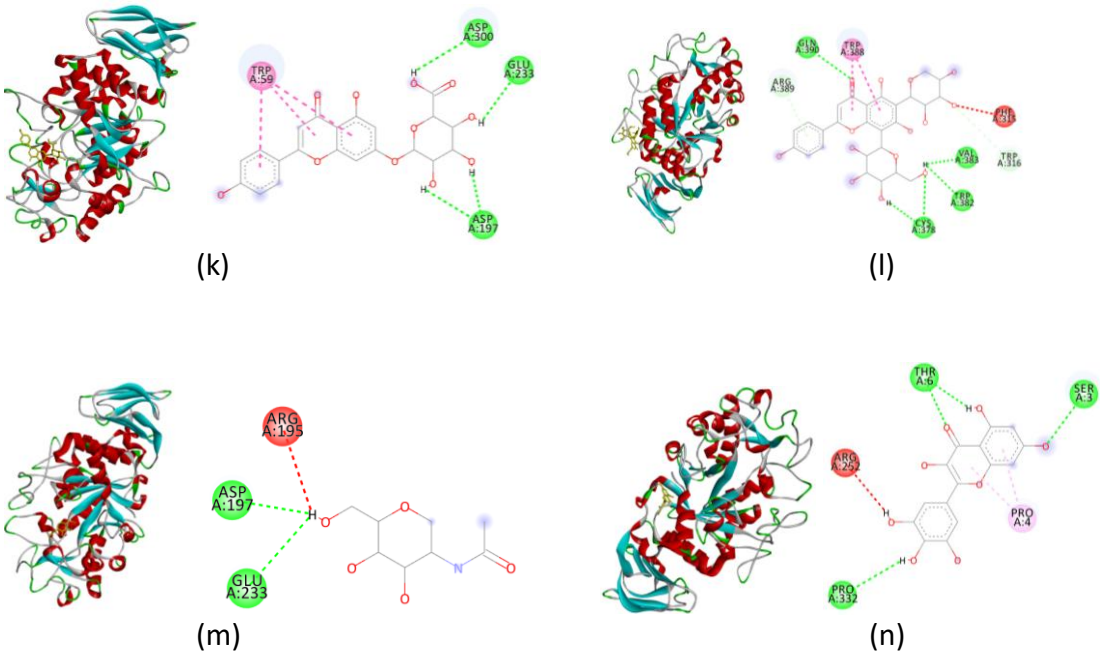

Figure 2. Visualization 3D (a) and 2D (b) binding interaction of α-amylase (4GQR) with acarbose(a), miglitol(b), voglibose(c), reserpine(d), oleanolic acid(e), coumaric acid(f), apigenin(g), glycitein(h), flurandrenolide(i), scuttelarin(j), apigenin-7-*O*-glucoronide(k), corymboside(l), GLC(m), and MYC (n).

The binding affinity between the ligand isolated from *A. ilicifolius* leaves and the receptor α-amylase (PDB ID: 4GQR) ranged from -6.1 to -9.3 kcal/mol. The binding affinities of the ligands, miglitol, voglibose, and acarbose, to the receptor were -5.2, -6.4, and -8.3 kcal/mol, respectively. The component with the most binding affinity to the receptor among the discovered compounds from *A. ilicifolius* leaves extract was corymboside, with a binding energy of -9.3 kcal/mol. On the other hand, the molecular docking between 4-coumaric acid and the receptor resulted in the lowest binding affinity of -6.1 kcal/mol. Among the ligands, scuttelarin, apigenin-7-glucuronide, corymboside, and oleanolic acid had binding affinities with values higher than -9 kcal/mol, namely -9.1 kcal/mol and -9.9 kcal/mol.

The molecular interaction between α-amylase and ligands is illustrated in Figure 2 and summarized in Table 3. According to the visualization, the hydrogen bond interactions with NAG (native ligands) included two specific amino acid residues: Asp197 and Glu233. The structure of human pancreatic α-amylase (HPA) consists of three domains, with the active sites located at Asp197, Glu233, and Asp300. The active site facilitates the hydrolysis of glycosidic bonds by certain catalytic residues. For example, Asp197 acts as a nucleophile, Glu233 acts as an acid or base, and Asp300 optimizes the orientation of the substrate and stabilizes the transition state (55–57). The study clearly demonstrates the molecular interactions between various ligands and specific amino acid residues. For instance, reserpine binds to Asp197 and Asp300, oleanolic acid binds to Asp197 and Glu233, 4-coumaric acid binds to Asp197, apigenin binds to Asp197, Glu233, and Asp300, glycitein binds to Asp197 and Asp300, flurandrenolide binds to Asp197, scuttelarin binds to Asp197 and Glu233, and apigenin-7-glucoronide binds to Asp197, Glu233, and Asp200.

The investigations revealed the significant role of hydrogen bonds in ligand binding to α-amylase. The compounds found in the *A. ilicifolius* extract demonstrated a stronger binding affinity with both the α-glucosidase and α-amylase receptors, when compared to acarbose. The study found that the extract from A. *ilicifolius* leaves is highly effective in inhibiting the

activity of α-glucosidase and α-amylase. ASP197 and GLU233 are part of the catalytic triad of alpha-amylase and are involved in hydrogen bonding with inhibitors. ASP300 contribute as a stabilizer for the transition state and is targeted by polar groups of inhibitors. The top inhibitors interact with these residue by occupying the active site and forming stable hydrogen bonds with residues essential for catalysis, thereby blocking substrate access and inhibiting enzymatic activity.

3.3. Drug-likeness and Toxicity

Natural products are widely recognized for their abundance of biologically active substances. There has been a significant increase in the number of bioactive compounds being introduced to the market, either as herbal medicine or as functional food. The safety of natural-product-derived molecules was assessed by evaluating drug-likeness and toxicity, as shown in Table 4.

Table 4. Drug-likeness and Toxicity Analysis.

Compounds	Lipinski Rule	SWISS ADME		Toxicity	
		Bioavailability	Absorption	LD_{50} (mg/kg)	Level
Flurandrenolide	Yes	0.55	high	1,451	4
Corymboside	No	0.17	low	4,000	5
Scutellarin	Yes	0.11	low	5,000	5
Apigenin 7-O-glucuronide	Yes	0.55	high	5,000	5
Luteolin	Yes	0.55	high	3,919	5
Glycitein	Yes	0.55	high	2,500	5
Reserpine	No	0.17	high	300	3
Apigenin	Yes	0.55	high	2,500	5
4-Coumaric acid	Yes	0.85	high	2,850	5
Oleanolic acid	Yes	0.85	low	2,000	4

The concept of drug-likeness was derived from a series of evaluations of physicochemical characteristics and/or the structure of organic chemistry or drug candidates. It is employed to identify undesirable elements of compounds as a whole, such as low ADMET value (58,59). This study assessed drug-likeness based on the Lipinski Rule, Swiss ADME, and toxicity. The drug-likeness and toxicity assessments were presented in Table 4. The toxicity and toxicity class of the identified chemicals in the *A. ilicifolius* leaves extract were assessed. The criteria for selecting a compound as a candidate drug include its safety and absence of toxicity. Based on Table 4, it can be concluded that all the chemicals detected in the *A. ilicifolius* leaves extract are safe for consumption, as none of them belong to class or level 1. Class 1 fatal if swallowed ($LD_{50} \leq 5$), class II fatal if swallowed ($5 < LD_{50} \leq 50$), class III toxic if swallowed ($50 < LD_{50} \leq 300$), class IV dangerous if swallowed ($300 < LD_{50} \leq 2000$), class V may be dangerous if swallowed ($2000 < LD_{50} \leq 5000$) and class VI if LD_{50} >5000 (37).

4. Conclusions

This study identified various phytochemical compounds present in the extract of *A. ilicifolius* leaves. These compounds include steroid (flurandrenolide), terpenoids (oleanolic acid), alkaloid (reserpine), and flavonoids (corymboside, scutellarin, apigenin 7-O-glucuronide, luteolin, glycitein, apigenin, 4-coumaric acid, p-coumaric acid glucose, apigenin

glucuronide, biochanin A -8-C-glucose, luteolin glucuronide, quercetin, apigenin glucose-glucose). Research findings indicate that three compounds, namely reserpine, scuttelarin, and apigenin-7-glucuronide, exhibit higher energy binding than other ligands. Reserpine has a binding energy of -10 kkal/mol, while scuttelarin and apigenin-7-glucuronide both have a binding energy of -9.9 kkal/mol. The molecular interaction between α-amylase and four compounds found in *A. ilicifolius* leaves extract, including corymboside, apigenin-7-glucuronide, scutellarin, and oleanolic acid, exhibits a higher binding affinity. Based on the findings, it can be inferred that the extract from *A. ilicifolius* leaves has the ability to effectively inhibit the activity of α-glucosidase and α-amylase, as determined through *in silico* methods While toxicity classification provides a useful starting point for assessing drug safety, it is not sufficient to conclude that a compound is safe for consumption as a food ingredient. Therefore, future investigations should include both in vitro and in vivo analyses to determine the Acceptable Daily Intake (ADI) of *A. ilicifolius* leaves. This will ensure that any proposed use in food products meets established safety standards for human consumption.

Acknowledgements

The research was financially supported by Lembaga Penelitian dan Pengabdian Masyarakat through the Hibah Penelitian Pemula 2023 program, with grant number 611.40/UN10.C200/2023.

Author Contributions

YEP, and HH were responsible for the experimental conception and design. YAS, NRD, LAP, and IPH conducted the experiments. YEP, TDS, AF and HH analyzed the data. AWP provided reagents and materials, while YEP authored the paper.

Institutional Review Board Statement

Not applicable

Data Availability Statement

The drug-likeness properties of A. ilicifolius leaves were assessed using Lipinski's rule and the SwissADME database (http://www.swissadme.ch/index.php). In addition, the toxicity level and LD50 were predicted using the Protox tool, which can be found at https://tox-new.charite.de/protox_II/. The 3D structure of the Ligand was obtained by downloading it in SDF format from the PubChem database (https://pubchem.ncbi.nlm.nih.gov). The native ligands, NAG and MYC, were obtained in SDF format from the Protein Data Bank (https://www.rcsb.org/). Furthermore, the molecular composition of ligand control, specifically acarbose, miglitol, and voglibose, was obtained in SDF format from the PubChem database (https://pubchem.ncbi.nlm.nih.gov). The crystal structures of α-glucosidase and α-amylase were obtained from the Protein Data Bank (PDB ID: 3A4A and PDB ID: 4GQR) (https://www.rcsb.org/) respectively. In addition, the ligands and water molecules were eliminated, and polar hydrogen was introduced to the protein receptor using Biovia Discovery Studio 2019.

Conflicts of Interest

Authors may declare no conflict of interest.

References

1. Priebe MG, Eelderink C, Wachters-Hagedoorn RE, Vonk RJ. Starch Digestion and Applications of Slowly Available Starch. In: Sjoo M, Nilsson L, editors. Starch in Food: Structure, Function and Applications: Second Edition [Internet]. Second. Cambridge: Woodhead Publishing; 2018. p. 805–26. Available from: https://www.elsevier.com/books/starch-in-food/sjoo/978-0-08-100868-3
2. Derosa G, Maffioli P. α-Glucosidase inhibitors and their use in clinical practice. Vol. 8, Archives of Medical Science. 2012. p. 899–906.
3. Fujisawa T, Ikegami H, Inoue K, Kawabata Y, Ogihara T. Effect of two α-glucosidase inhibitors, voglibose and acarbose, on postprandial hyperglycemia correlates with subjective abdominal symptoms. Metabolism. 2005;54(3):387–90.
4. Zhang K, Chen XL, Zhao X, Ni JY, Wang HL, Han M, et al. Antidiabetic potential of Catechu via assays for α-glucosidase, α-amylase, and glucose uptake in adipocytes. J Ethnopharmacol. 2022;291:1–10.
5. Bastos KX, Dias CN, Nascimento YM, Da Silva MS, Langassner SMZ, Wessjohann LA, et al. Identification of phenolic compounds from hancornia speciosa (apocynaceae) leaves by UHPLC Orbitrap-HRMS. Molecules. 2017;22(1).
6. Zhang L, Xu L, Ye Y hua, Zhu M fang, Li J, Tu Z cai, et al. Phytochemical profiles and screening of α-glucosidase inhibitors of four Acer species leaves with ultra-filtration combined with UPLC-QTOF-MS/MS. Ind Crops Prod. 2019;129(129):156–68.
7. Amin A, Hanif M, Rafey A, Zaib S, Bakhsh S, Ramzan M, et al. Sesquiterpene Coumarins from Ferula narthex 15-LOX, α-Glucosidase Inhibition and Molecular Docking Studies. Vol. 30, Revista Brasileira de Farmacognosia. 2020. p. 12–7.
8. Li S, Zhang W, Wang R, Li C, Lin X, Wang L. Screening and identification of natural α-glucosidase and α-amylase inhibitors from partridge tea (Mallotus furetianus Muell-Arg) and in silico analysis. Food Chem. 2022;388:1–10.
9. Sichaem J, Aree T, Lugsanangarm K, Tip-Pyang S. Identification of highly potent α-glucosidase inhibitory and antioxidant constituents from Zizyphus rugosa bark: Enzyme kinetic and molecular docking studies with active metabolites. Pharm Biol. 2017;55(1):1436–41.
10. Zheng Q, Jia R bo, Luo D, Lin L, Chen C, Zhao M. The effect of extraction solution pH level on the physicochemical properties and α-glucosidase inhibitory potential of Fucus vesiculosus polysaccharide. LWT - Food Sci Technol. 2022;169(May):1–11.
11. Kim KY, Nam KA, Kurihara H, Kim SM. Potent α-glucosidase inhibitors purified from the red alga Grateloupia elliptica. Phytochemistry. 2008;69:2820–5.
12. Bunyapraphatsara N, Srisukh V, Utiviboonsuk A, Sornlek P, Thongbainoi W, Chuakul W, et al. Vegetables From The Mangrove Areas. J Phytopharm. 2002;9(1).
13. Bibi SN, Fawzi MM, Gokhan Z, Rajesh J, Nadeem N, Rengasamy Kannan RR, et al. Ethnopharmacology, Phytochemistry, and Global Distribution of Mangroves-A Comprehensive Review. Mar Drugs. 2019;17(231).
14. Puspitasari YE, Tampubolon HO, Fajrin AN, Sulistiyati TD, Hardoko H. Penghambatan α -Glucosidase Oleh Flavonoid Dari Ekstrak Etil Asetat Daun Mangrove Sonneratia alba Sebagai Antidiabetes Melalui Penambatan Molekuler Inhibition of α -Glucosidase by Flavonoid Prepared from Ethyl Acetate Extract of Sonneratia alba Leaves as . Saintek Perikan Indones J Fish Sci Technol. 2023;19(1):15–22.

15. Puspitasari YE, Hardoko H, Sulistiyati TD, Fajrin NA, Tampubolon HO. Identifikasi Senyawa Fitokimia dari Daun Mangrove Sonneratia alba dan Analisis in Silico Sebagai Antidiabetes (Phytochemical Compound Identification of Mangrove Leaves Sonneratia alba and in Silico Analysis as Antidiabetic). J Perikan dan Kelaut. 2022;27(2):241–8.
16. Hardoko, Sasmito BB, Puspitasari YE. Tannin extract characterization of young mangrove Rhizophora mucronata leaves as ingredients for diabetic functional food. Asian J Microbiol Biotechnol Environ Sci. 2017;19(2):331–6.
17. Hardoko, Hafidz AY, Sasmito BB, Halim Y. Antidiabetic Potency and Characteristics of Corn Flour and Cassava Flour-Based Rice Analog Added with Rhizophora mucronata Mangrove Fruit Flour and Euchema cottoni Seaweed Flour. In: Proceeding 5th International Conference on Food, Agriculture and Natural Resources 2019. 2019. p. 199–204.
18. Hardoko H, Sasmito BB, Puspitasari YE. Antidiabetic and antioxidant activities of tannin extract of Rhizophora mucronata leaves. J Chem Pharm Res. 2016;8(3):143–8.
19. Hardoko, Harisman EK, Puspitasari YE. The kombucha from Rhizophora mucronata Lam . herbal tea : Characteristics and the potential as an antidiabetic beverage. J Pharm Pharm Res. 2020;8(137):410–21.
20. Nindhia TS, Nindhia, Trisnawati NN. Data on Potential of Indonesian variety of Sea holly (Acanthus ilicifolius Linn) as Herbal Medicine. ACM Int Conf Proceeding Ser. 2020;52–6.
21. Kanchanapoom T, Kamel MS, Kasai R, Picheansoonthon C, Hiraga Y, Yamasaki K. Benzoxazinoid glucosides from Acanthus ilicifolius. Phytochemistry. 2001;58(4):637–40.
22. Kanchanapoom T, Kamel MS, Kasai R, Yamasaki K, Picheansoonthon C, Hiraga Y. Lignan glucosides from Acanthus ilicifolius. Phytochemistry. 2001;56(4):369–72.
23. Wu J, Zhang S, Xiao Q, Li Q, Huang J, Long L, et al. Megastigmane and flavone glycosides from Acanthus ilicifolius. Pharmazie. 2003;58:363–4.
24. Wu J, Zhang S, Li Q, Huang J, Xiao Z, Long L. Two new cyclolignan glycosides from Acanthus ilicifolius. Zeitschrift fur Naturforsch - Sect B J Chem Sci. 2004;59(3):341–4.
25. Huo C, Liang H, Tu G, Zhao Y, Lin W. A new 5,11-epoxymegastigmane glucoside from Acanthus ilicifolius. Nat Prod Res. 2008;22(10):896–900.
26. Huang MY, Zhong LJ, Wang F, Liu QY, Zhang YH. Chemical constituents from the roots of Acanthus ilicifolius var. xiamenensis. Biochem Syst Ecol. 2014;55:145–7.
27. Cai YS, Sun JZ, Tang QQ, Fan F, Guo YW. Acanthiline A, a pyrido[1,2-a]indole alkaloid from Chinese mangrove Acanthus ilicifolius. J Asian Nat Prod Res. 2018;20(11):1088–92.
28. Wu J, Zhang S, Xiao Q, Li Q, Huang J, Long L, et al. Phenylethanoid and aliphatic alcohol glycosides from Acanthus ilicifolius. Phytochemistry. 2003;63(4):491–5.
29. Wu J, Zhang S, Huang J, Xiao Q, Li Q, Long L, et al. New aliphatic alcohol and (Z)-4-coumaric acid glycosides from Acanthus ilicifolius. Chem Pharm Bull. 2003;51(10):1201–3.
30. Nurfitri WA, Widiastuti EL, Cahyani EN. Efek Ekstrak Metanol Daun Jeruju (Acanthus ilicifolius L.) Serta Buah Jeruju Dan Taurin dalam Menurunkan Kadar Glukosa Darah Dan Kolesterol Serta Fertilitas Mencit Jantan (Mus musculus) Yang Diinduksi Aloksan. Pros Semin Nas Tumbuh Obat Indones ke-55. 2018;267–75.
31. Widiastuti EL, Ardiansyah BK, Nurcahyani N, Silvinia A. Antidiabetic Potency of Jeruju

(Acanthus ilicifolius L.) Ethanol Extract and Taurine on Histopathological Response of Mice Kidney (Mus musculus L.) Induced by Alloxan. J Phys Conf Ser. 2021;1751(1).
32. Derebe D, Wubetu M, Alamirew A. Hypoglycemic and antihyperglycemic activities of 80% methanol root extract of acanthus polystachyus delile (Acanthaceae) in type 2 diabetic rats. Clin Pharmacol Adv Appl. 2020;12:149–57.
33. Ogundajo A, Kazeem M, Owoyele O, Ogunmoye A, Ogunwande I. Inhibition of α-amylase and α-glucosidase by Acanthus montanus Leaf Extracts. Vol. 9, British Journal of Pharmaceutical Research. 2016. p. 1–8.
34. Somtimuang C, Olatunji OJ, Ovatlarnporn C. Evaluation of In Vitro α-Amylase and α-Glucosidase Inhibitory Potentials of 14 Medicinal Plants Constituted in Thai Folk Antidiabetic Formularies. Chem Biodivers. 2018;15(4).
35. Daina A, Michielin O, Zoete V. SwissADME: A free web tool to evaluate pharmacokinetics, drug-likeness and medicinal chemistry friendliness of small molecules. Sci Rep [Internet]. 2017;7(January):1–13. Available from: http://dx.doi.org/10.1038/srep42717
36. Drwal MN, Banerjee P, Dunkel M, Wettig MR, Preissner R. ProTox: A web server for the in silico prediction of rodent oral toxicity. Nucleic Acids Res. 2014;42(W1):53–8.
37. Banerjee P, Eckert AO, Schrey AK, Preissner R. ProTox-II: A webserver for the prediction of toxicity of chemicals. Nucleic Acids Res. 2018;46(W1):W257–63.
38. Sivakumar K, Kannappan S, Vijayakumar B, Jithendran KP, Balasubramaniam S, Panigrahi A. Molecular docking study of bio-inhibitors extracted from marine macro-alga Ulva fasciata against hemolysin protein of luminescence disease-causing Vibrio harveyi. Arch Microbiol. 2021;203(7):4243–58.
39. Saranya A, Ramanathan T, Kesavanarayanan KS, Adam A. Traditional Medicinal Uses , Chemical Constituents and Biological Activities of a Mangrove Plant , Acanthus ilicifolius Linn . : A Brief Review. Am J Agric Environ Sci. 2015;15(2):243–50.
40. Jaiwal B V., Shaikh FK, Bradosty SW, Patil AB, Hallur RLS. Identification of matrix metalloproteinases inhibitors from methanol extract of Peltophorum pterocarpum leaves. J Appl Biol Biotechnol. 2023;11(4):92–8.
41. Anand J, Anil B. Phytochemical screening of Rhizome extract of Curcuma zedoaria (Christm) Roscoe by HRLC-MS technique. Int J Life Sci [Internet]. 2019;7817(December):53–7. Available from: http://www.ijlsci.in
42. Singh UP, Gahtori P. Therapeutic potential of Reserpine in metabolic syndrome : An evidence based study. Pharmacol Res. 2023;190(October):0–3.
43. Panwar GS, Guru SK. Stimulation of reserpine production in the whole plant culture of Rauwolfia serpentina L. by elicitors and precursor feeding. J Plant Biochem Biotechnol. 2015;24(1):49–55.
44. Lobay D. Rauwolfia in the Treatment of Hypertension. Integr Med. 2015;14(3):40–6.
45. Besson E, Dombris A, Raynaud J, Chopin J. Corymboside, nouvelle di-c-glycosylflavone racines de Carlina corymbosa. Phytochemistry. 1979;18:1899–900.
46. Wang J, Tan J, Luo J, Huang P, Zhou W, Chen L, et al. Enhancement of scutellarin oral delivery efficacy by vitamin B12-modified amphiphilic chitosan derivatives to treat type II diabetes induced-retinopathy. J Nanobiotechnology. 2017;15(1):1–17.
47. Zhang Z feng, Lu L yang, Liu Y. A New Procedure for Separation and Purification of Scutellarin from Erigeron multiradiatus. Chinese Herb Med [Internet]. 2013;5(2):133–7. Available from:

http://www.sciencedirect.com/science/article/pii/S1674638413600209%5Cnhttp://ac.els-cdn.com/S1674638413600209/1-s2.0-S1674638413600209-main.pdf?_tid=c4b94718-ddc4-11e2-8322-00000aab0f02&acdnat=1372184976_ce3b53268ac945ab87dd9ce692a83cac

48. Yao H, Li S, Hu J, Chen Y, Huang L, Lin J, et al. Chromatographic fingerprint and quantitative analysis of seven bioactive compounds of Scutellaria barbata. Planta Med. 2011;77(4):388–93.
49. Haguet Q, Joubioux F Le, Chavanelle V, Groult H, Schoojans N, Langhi C, et al. Inhibitory Potential of α-Amylase, α-Glucosidase, and Pancreatic Lipase by a Formulation of Five Plant Extracts: TOTUM-63. Int J Mol Sci. 2023;24(3652):1–19.
50. Sadeghi M, Moradi M, Madanchi H, Johari B. In silico study of garlic (Allium sativum L.)-derived compounds molecular interactions with α-glucosidase. Silico Pharmacol. 2021;9(1).
51. Nipun TS, Khatib A, Ibrahim Z, Ahmed QU, Redzwan IE, Saiman MZ, et al. Characterization of α-Glucosidase Inhibitors from Psychotria malayana Jack Leaves Extract Using LC-MS-Based Multivariate Data Analysis and In-Silico Molecular Docking. Molecules [Internet]. 2020;25:1–17. Available from: www.mdpi.com/journal/molecules
52. Yamamoto K, Miyake H, Kusunoki M, Osaki S. Crystal structures of isomaltase from Saccharomyces cerevisiae and in complex with its competitive inhibitor maltose. FEBS J. 2010;277(20):4205–14.
53. Wu L, Liu Y, Qin Y, Wang L, Wu Z. HPLC-ESI-qTOF-MS/MS characterization, antioxidant activities and inhibitory ability of digestive enzymes with molecular docking analysis of various parts of raspberry (Rubus ideaus L.). Antioxidants. 2019;8(8):1–18.
54. Udrea AM, Pircalabioru GG, Boboc AA, Mares C, Dinache A, Mernea M, et al. Advanced bioinformatics tools in the pharmacokinetic profiles of natural and synthetic compounds with anti-diabetic activity. Biomolecules. 2021;11(11):1–31.
55. Williams LK, Li C, Withers SG, Brayer GD. Order and disorder: Differential structural impacts of myricetin and ethyl caffeate on human amylase, an antidiabetic target. J Med Chem. 2012;55(22):10177–86.
56. Brayer GD, Sidhu G, Maurus R, Rydberg EH, Braun C, Wang Y, et al. Subsite mapping of the human pancreatic α-amylase active site through structural, kinetic, and mutagenesis techniques. Biochemistry. 2000;39(16):4778–91.
57. Casacchia T, Occhiuzzi MA, Grande F, Rizzuti B, Granieri MC, Rocca C, et al. A pilot study on the nutraceutical properties of the Citrus hybrid Tacle® as a dietary source of polyphenols for supplementation in metabolic disorders. J Funct Foods. 2019;52(October 2018):370–81.
58. Tian S, Wang J, Li Y, Li D, Xu L, Hou T. The application of in silico drug-likeness predictions in pharmaceutical research. Adv Drug Deliv Rev. 2015;86:2–10.
59. Lipinski CA, Lombardo F, Dominy BW, Feeney PJ. Experimental and computational approaches to estimate solubility and permeability in drug discovery and development settings. Adv Drug Deliv Rev. 1997;23:3–25.